NATIONAL ADVISORY COMMITTEE FOR AERONAUTICS

WARTIME REPORT

ORIGINALLY ISSUED
May 1943 as
Advance Restricted Report 3E24

METHOD OF CALCULATING PERFORMANCE OF DUAL-ROTATING PROPELLERS FROM AIRFOIL CHARACTERISTICS

By Irven Naiman

Langley Memorial Aeronautical Laboratory
Langley Field, Va.

WASHINGTON

NATIONAL ADVISORY COMMITTEE FOR AERONAUTICS

ADVANCE RESTRICTED REPORT

METHOD OF CALCULATING PERFORMANCE OF DUAL-ROTATING PROPELLERS FROM AIRFOIL CHARACTERISTICS

By Irven Naiman

SUMMARY

A method is developed for calculating the performance of a dual-rotating propeller from the section characteristics of the blade elements. The method is applied to an eight-balde dual-rotating propeller and the computed results are compared with low-speed wind-tunnel tests of the same propeller in both the tractor and the pusher positions. The computations are found to agree within the experimental accuracy of the measurements. A detailed step-by-step procedure for the computations is given in an appendix.

INTRODUCTION

The work of Betz, Prandtl, Goldstein, and Lock has advanced propeller theory to the point at which performance may be calculated with considerable confidence from section characteristics. With the introduction of dual-rotating propellers, an extension of the methods to this type was desirable. An exact, potential-theory solution corresponding to that of Goldstein has not as yet been obtained. Several approximations, however, covering specific phases of the problem have appeared. Lock (reference 1) replaces the pulsating-velocity field by one of a steady, average value. In this way equations are obtained by which the performance may be calculated. Collar (references 2 and 3) by cascade theory obtains some of the periodic effects.

The equations of reference 1 are very lengthy and cumbersome and the cross interpolation required for the solution makes the actual computation very tedious; for this reason several approximations that provide a quicker solution at lower accuracy are given. In the present paper,

by a different method based upon the same assumptions used in reference 1, new equations are obtained providing a simpler and faster computation for the necessary degree of accuracy.

In appendix A a complete outline of the method of computation for dual-rotating propellers is given. The procedure may be followed without reference to the derivation given in the text, and specimen computations are included. The necessary calculations for the single-rotating propeller may be easily performed by the same method.

Throughout the rest of this paper, dual-rotating propeller will be referred to as "dual propeller" and single-rotating propeller as "single propeller."

SYMBOLS

A $A'\omega$

A' average value of rotational inflow factor of front propeller $\left(\frac{F_1 \tan \epsilon_1}{\cot \varphi_1 + \tan \epsilon_1}\right)$

B number of blades per propeller

c chord of propeller blade element

C_D section drag coefficient $\left(\frac{D}{1/2\ \rho W^2 c}\right)$

C_L section lift coefficient $\left(\frac{L}{1/2\ \rho W^2 c}\right)$

C_X section axial-force coefficient $\left(\frac{X}{1/2\ \rho W^2 c}\right)$

C_Y section tangential-force coefficient $\left(\frac{Y}{1/2\ \rho W^2 c}\right)$

C_P propeller power coefficient $\left(\frac{P}{\rho n^3 D^5}\right)$

C_Q propeller torque coefficient $\left(\frac{Q}{\rho n^2 D^5}\right)$

C_T propeller thrust coefficient $\left(\frac{T}{\rho n^2 D^4}\right)$

D drag at blade element; except, propeller diameter in C_P, C_Q, C_T, and J

F correction factor for finite number of blades

G computational quantity (equation (21))

J advance-diameter ratio $\left(\frac{V}{nD}\right)$

K Goldstein circulation function

L lift at blade element

n rotational speed of propeller (revolutions/unit time)

P power of propeller ($2\pi nQ$)

Q torque of propeller

r radius to propeller blade element

R radius to tip of propeller

T thrust of propeller

u average induced axial velocity at one propeller due to other propeller

v average induced tangential velocity at one propeller due to other propeller

V advance velocity of propeller

w self-induced velocity at propeller

W resultant velocity of propeller

x proportional radius of blade element $\left(\frac{r}{R}\right)$

X axial force at blade element

Y tangential force at blade element

α angle of attack

β propeller blade angle at 0.75R

γ drag-lift angle $\left(\tan \gamma = \frac{C_D}{C_L}\right)$

ϵ induced increase in angle of inflow $\left(\tan \epsilon = \frac{w}{V}\right)$

η_x propeller section efficiency

θ propeller blade angle at radius r

ρ density of air

σ solidity per propeller $\left(\frac{Bc}{2\pi r}\right)$

φ angle of resultant velocity W to plane of rotation

φ_o advance angle of blade element $\left(\tan \varphi_o = \frac{V}{r\Omega}\right)$

φ_o' effective advance angle of blade element due to induced velocity of other propeller (equation (12))

Ω angular velocity of propeller $(2\pi n)$

ω ratio of angular velocities of front to rear propeller $\left(\frac{\Omega_1}{\Omega_2}\right)$

Subscripts:

1 front propeller

2 rear propeller

THEORETICAL CONSIDERATIONS

Assumptions

The theory of propeller operation has been developed from several assumptions that may well be summarized here. The fundamental simplifying assumption of all propeller strip-theory calculations is that the operation at any radial element is independent of that at any other element. Goldstein (reference 4) obtained the exact frictionless solution for the lightly loaded propeller with a finite number of blades and minimum energy loss. He introduced a nondimensional quantity K specifying the distribution of circulation. Because of the finite number of blades, the velocity distribution at any radius is not uniform. The correct value of the induced velocity to be used in determining the lift relationship is the value at the blade, that is, the value on the vortex sheet. This relationship between the lift coefficient and the induced velocity is given by

$$\sigma C_L = 4F \sin\varphi \tan\epsilon \qquad (1)$$

where $F = \frac{K}{\cos^2\varphi}$ and $\tan\epsilon = \frac{w}{W}$, φ is the pitch angle of the vortex sheet, w is the induced velocity normal to the vortex sheet, and W is the resultant velocity of the blade element along the sheet. Strictly speaking, F (κ in the notation of reference 1) is applicable only to lightly loaded propellers with a distribution of circulation giving minimum energy loss. Because a perfectly general solution to this problem is lacking, the following assumption is made: The factor F may be applied as a first approximation for nonoptimum distributions and heavy loadings. Equation (1) represents a further assumption: The frictional losses have negligible effect upon the induced losses, appearing merely as modifications in the wake in the immediate neighborhood of the vortex sheets.

In the dual propeller, each propeller operates in the nonuniform velocity field of the other propeller, resulting in an oscillation in the angle of attack and in the magnitude of the velocity. Lock makes the following assumptions:

(1) The oscillating induced-velocity field may be replaced by a uniform field, the value for which is equal to the mean value of the oscillating field.

(2) The mean value of the induced velocity is taken to be F times the value induced at the vortex sheet.

(3) Because a general solution for the dual propeller is lacking, the self-induced velocities are determined in the same way as for a single propeller; that is, the value of F is that for single propellers.

(4) The propellers are assumed to be sufficiently close together that changes in axial velocity between them are negligible.

Statement of Propeller Problem in General Form

The problem of propeller-performance computation resolves into determining the lift and the drag on a propeller with a given number of blades, certain airfoil sections, solidity, and blade-angle setting at a known value of the advance-diameter ratio. The correct resolution of the lift and the drag into thrust and torque requires that the direction of the inflow velocities, or the pitch angle of the vortex sheet φ, be known. The lift coefficient is a function of the angle of attack α, which is equal to $\theta - \varphi$; that is,

$$C_L = M(\theta - \varphi) \tag{2}$$

The loading of the propeller is a function of the pitch and of the magnitude of the induced velocities of the vortex sheet, as given by equation (1). For the single propeller, $\epsilon = \varphi - \varphi_o$, with the result that

$$\sigma C_L = 4F \sin \varphi \tan (\varphi - \varphi_o) \tag{3}$$

If equations (2) and (3) are combined, the general propeller equation may therefore be written

$$M(\theta - \varphi) = \frac{4F}{\sigma} \sin \varphi \tan (\varphi - \varphi_o)$$

or, symbolically,

$$\Phi(\theta, \varphi, \varphi_o) \equiv M(\theta - \varphi) - \frac{4F}{\sigma} \sin \varphi \tan (\varphi - \varphi_o) = 0 \qquad (4)$$

The function Φ properly includes σ and B as additional variables but, because these quantities are usually fixed by other considerations, they may here be considered as included with θ.

If the propeller is working not in free air but in an air stream that has been modified by body interference, body wake, or slipstream of another propeller, the advance angle φ_o' appropriate to these conditions must be used instead of φ_o:

$$\Phi(\theta, \varphi, \varphi_o') = 0$$

For the dual propeller, two such functions exist

$$\left.\begin{aligned} \Phi(\theta_1, \varphi_1, \varphi_o'_1) &= 0 \\ \Phi(\theta_2, \varphi_2, \varphi_o'_2) &= 0 \end{aligned}\right\} \qquad (5)$$

where $\varphi_o'_1$ and $\varphi_o'_2$ are functions of the slipstream effect of the other propeller. The simultaneous solution of these two equations is desired. The process, of course, can be generalized to any number of propellers operating in series.

The general propeller function Φ is a function of three variables. If any two of these variables are selected, the third may be found. In computing the performance of a given propeller, θ (and σ and B) is given and the thrust and the torque are desired. The normal approach is to compute the thrust and the torque for an arbitrarily selected value of the advance-diameter ratio J. With θ and φ_o selected, φ is therefore determined from equation (4) and the lift, the thrust, and the torque follow. For the dual propeller, two sets of values are

required, one for each propeller. By repeating the process for other values of J, the complete performance curve may be obtained. This method was used in reference 1. The equations are long and involved and the necessary cross interpolation makes the actual computation quite tedious.

An alternative method is presented by examination of equation (4). If φ is selected arbitrarily instead of φ_o, φ_c is very easily determined. An arbitrary value of C_L may be assumed and φ may be determined by use of the lift curve, or vice versa. The corresponding value of J is then found. The complete performance curve for each station is constructed and the value at any desired value of J is thus obtained. This method requires considerably less computational work than the preceding method. By this second method very little more computation is required for dual propellers than for single propellers; most of the additional work is that necessary for computing the additional coefficients for the second propeller.

ANALYSIS

The Interference Velocities

In accordance with the preceding assumptions the interference velocities may be expressed as follows:

The velocity diagram for a propeller working in the field of another propeller is given in figure 1. The self-induced velocity w is perpendicular to the resultant velocity W, which makes an angle φ with the plane of rotation. This diagram is similar to the diagram for single propellers except for the introduction of the additional velocities u and v, the effective values of the axial and rotational interference velocities of the other propeller.

The additional axial velocity for each propeller due to the other is the average value of that induced at the other propeller. The additional rotational velocity for the front propeller due to the rear propeller is nil; for the rear propeller due to the front propeller, the velocity is twice the average value of the velocity induced at the front propeller. Thus

$$\left.\begin{aligned} u_1 &= F_2 w_2 \cos \varphi_2 \\ u_2 &= F_1 w_1 \cos \varphi_1 \\ v_1 &= 0 \\ v_2 &= 2F_1 w_1 \sin \varphi_1 \end{aligned}\right\} \tag{6}$$

In nondimensional form these velocities become (see appendix B)

$$\frac{u_1}{r\Omega_2 + v_2} = \frac{F_2 \tan \epsilon_2}{1 + \tan \varphi_2 \tan \epsilon_2} \tag{7}$$

$$\frac{u_2}{r\Omega_2} = A \cot \varphi_1 \tag{8}$$

$$\frac{v_2}{r\Omega_2} = 2A \tag{9}$$

where

$$A = A'\omega \tag{10}$$

and

$$A' \equiv \frac{F_1 \tan \epsilon_1}{\cot \varphi_1 + \tan \epsilon_1} = 1/2 \frac{v_2}{r\Omega_1} \tag{11}$$

The factor A' is thus seen to be the mean value of the rotational inflow factor of the front propeller (a' in momentum theory).

Also

$$\frac{V + u_1}{r\Omega_1} = \tan (\varphi_1 - \epsilon_1) = \tan \varphi_0{}'_1 \tag{12}$$

$$\frac{V + u_2}{r\Omega_2 + v_2} = \tan (\varphi_2 - \epsilon_2) = \tan \varphi_0{}'_2 \qquad (13)$$

Solution for Dual Propellers

The general propeller functions (equations (5)) are independent except for the terms in φ_0'. The solution therefore depends upon determining the relationship between $\varphi_0{}'_1$ and $\varphi_0{}'_2$. This solution may be carried out in the following manner.

The mean axial flow through both propellers is the same; thus,

$$V + u_1 + u_2 = V + u_2 + u_1 \qquad (14)$$

Now,

$$r\Omega_2 + v_2 = r\Omega_1(1 + 2A)/\omega \qquad (15)$$

Dividing the left-hand member of equation (14) by $r\Omega_1(1 + 2A)/\omega$ and the right-hand member by $r\Omega_2 + v_2$ gives

$$\frac{1}{1 + 2A}\left[\omega\left(\frac{V + u_1}{r\Omega_1}\right) + \frac{u_2}{r\Omega_2}\right] = \frac{V + u_2}{r\Omega_2 + v_2} + \frac{u_1}{r\Omega_2 + v_2}$$

By equations (7) to (13),

$$\frac{1}{1 + 2A}(\omega \tan \varphi_0{}'_1 + A \cot \varphi_1) = \tan \varphi_0{}'_2 + \frac{F_2 \tan \epsilon_2}{1 + \tan \varphi_2 \tan \epsilon_2} \qquad (16)$$

Now,

$$\tan \varphi_0{}'_1 = \frac{V + u_1}{r\Omega_1} = \frac{V}{r\Omega_1} + \frac{u_1(1 + 2A)}{\omega(r\Omega_2 + v_2)}$$

$$= \tan \varphi_{01} + \frac{1 + 2A}{\omega} \frac{F_2 \tan \epsilon_2}{1 + \tan \varphi_2 \tan \epsilon_2} \qquad (17)$$

Similarly,

$$\tan \varphi_0{}'_2 = \frac{\tan \varphi_{02} + A \cot \varphi_1}{1 + 2A} \qquad (18)$$

Also,

$$\omega \tan \varphi_{01} = \tan \varphi_{02} \qquad (19)$$

Equations (16) to (19), with the following identity, permit the solution of the dual-propeller problem in several ways:

$$\tan \varphi_0{}' \equiv \tan (\varphi - \epsilon) \equiv \frac{\tan \varphi - \tan \epsilon}{1 + \tan \varphi \tan \epsilon} \qquad (20)$$

If $\tan \varphi_0{}'$ is eliminated in equations (17) and (18) by use of equation (20), two equations are obtained that may be solved for ϵ_1 and ϵ_2 in terms of φ_{01}, φ_{02}, φ_1, and φ_2. This method was used in reference 1 although the solution there does not involve the same trigonometric functions. As may be seen by inspection, with φ_{01} and φ_{02} specified, values of φ_1 and φ_2 must be assumed; the corresponding values of ϵ_1 and ϵ_2 computed; C_{L_1} plotted against φ_1 for several fixed values of φ_2; C_{L_2} plotted similarly; by cross interpolation, the values of φ_1 and φ_2 that satisfy the given θ_1 and θ_2 may be found. A minimum of four points must be computed to perform this cross interpolation.

If the alternative method of the preceding section is adopted, however, a value of C_{L_1} is selected and φ_1 and ϵ_1 immediately follow. The left-hand member of equation (16) is a function only of φ_1 and ϵ_1 and may be designated G.

$$G \equiv \frac{\omega \tan (\varphi_1 - \epsilon_1) + A \cot \varphi_1}{1 + 2A} \qquad (21)$$

By use of equation (20), equation (16) may be solved for $\tan \epsilon_2$.

$$\tan \epsilon_2 = \frac{\tan \varphi_2 - G}{1 - F_2 + G \tan \varphi_2} \qquad (22)$$

The correct value of φ_2 will give an ϵ_2 and a C_{L_2} that satisfy the blade setting θ_2. This value may be determined graphically by computations for two values of φ_2. With the correct value, the advance angles φ_{o1} and φ_{o2} follow from equations (18) and (19):

$$\omega \tan \varphi_{o1} = \tan \varphi_{o2} = (1 + 2A) \tan (\varphi_2 - \epsilon_2) - A \cot \varphi_1 \qquad (23)$$

Expressions for Differential Thrust, Differential Torque, and Efficiency

The force diagram for the propeller blade element is given in figure 2. The differential thrust and the differential torque are given by

$$dT = BX\, dr$$

$$dQ = BY\, r dr$$

where B is the number of blades and

$$X = L \cos \varphi - D \sin \varphi$$

$$Y = L \sin \varphi + D \cos \varphi$$

The differential thrust and the differential torque may be expressed in nondimensional form in a great many ways. The following equations give these coefficients in terms of the same trigonometric functions previously used. The development of these expressions may be found in appendix B.

$$\frac{dC_{T_1}}{dx} = \pi^3 x^3 \frac{F_1 \tan \epsilon_1 (\cot \varphi_1 - \tan \gamma_1)}{(\cot \varphi_1 + \tan \epsilon_1)^2} \qquad (24a)$$

$$\frac{dC_{T_2}}{dx} = \pi^3 x^3 \frac{F_2 \tan \epsilon_2 (\cot \varphi_2 - \tan \gamma_2)}{[(\cot \varphi_2 + \tan \epsilon_2)/(1+2A)]^2} \qquad (24b)$$

and

$$\frac{dC_{Q_1}}{dx} = \frac{\pi^3 x^4}{2} \frac{F_1 \tan \epsilon_1 (1 + \cot \varphi_1 \tan \gamma_1)}{(\cot \varphi_1 + \tan \epsilon_1)^2} \qquad (25a)$$

$$\frac{dC_{Q_2}}{dx} = \frac{\pi^3 x^4}{2} \frac{F_2 \tan \epsilon_2 (1 + \cot \varphi_2 \tan \gamma_2)}{[(\cot \varphi_2 + \tan \epsilon_2)/(1+2A)]^2} \qquad (25b)$$

It is readily seen that $\frac{dC_T}{dx} = \frac{2}{x} \cot (\varphi + \gamma) \frac{dC_Q}{dx}$

The section efficiency for each propeller is given by

$$\eta_x = \frac{V dT}{\Omega dQ} = \frac{J}{2\pi} \frac{dC_T/dx}{dC_Q/dx}$$

$$= \frac{J}{\pi x} \cot (\varphi + \gamma)$$

$$= \tan \varphi_o \cot (\varphi + \gamma)$$

Special Case – Equal Rotational Speed and Equal Torque at Each Section

Equal rotational speed.– At equal rotational speed $\Omega_1 = \Omega_2 = \Omega$ and $\omega = 1$. Also $\tan \varphi_{o1} = \tan \varphi_{o2} = \tan \varphi_o$.

Equal torque.– Equal torque at the propeller blades implies zero average angular momentum in the wake; that is, the average angular velocity produced by each propeller is equal and opposite. This equality of velocity may be expressed by

$$F_1 w_1 \sin \varphi_1 = F_2 w_2 \sin \varphi_2$$

Dividing both terms by $r\Omega$ and applying the relationships of equations (7), (8), (9), (11), and (15) gives

$$\frac{F_1 \tan \epsilon_1}{\cot \varphi_1 + \tan \epsilon_1} = \frac{F_2 \tan \epsilon_2 (1 + 2A)}{\cot \varphi_2 + \tan \epsilon_2} \qquad (26)$$

Setting $dC_{Q_1}/dx = dC_{Q_2}/dx$ in equations (25) and using equation (26) gives as the necessary condition for equal torque, when frictional effects are neglected ($\gamma = 0$):

$$F_1 \tan \epsilon_1 = F_2 \tan \epsilon_2 \qquad (27)$$

From the lift relationship of equation (1), the condition for equal torque is

$$C_{L_1}/\sin \varphi_1 = C_{L_2}/\sin \varphi_2 \qquad (28)$$

From equations (26) and (27),

$$\cot \varphi_2 + \tan \epsilon_2 = (\cot \varphi_1 + \tan \epsilon_1)(1 + 2A)$$

$$= \cot \varphi_1 + (1 + 2F_1) \tan \epsilon_1$$

Then

$$\tan \epsilon_2 = \cot \varphi_1 + (1 + 2F_1) \tan \epsilon_1 - \cot \varphi_2$$

and, from equation (27),

$$F_2 = \frac{F_1 \tan \epsilon_1}{\cot \varphi_1 + (1 + 2F_1) \tan \epsilon_1 - \cot \varphi_2} \qquad (29)$$

With φ_1 and ϵ_1 determined, a value of φ_2 may be selected and F_2 may be calculated by equation (29).

This value is compared with the value of F_2 corresponding to φ_2 on the F-chart. (See fig. 14 or 15.) New values of φ_2 are selected and other values of F_2 are calculated until agreement is reached. In practice this method is found to be very rapidly convergent.

Difference in blade-angle settings for equal torque.- The correct difference in blade-angle setting is the difference that gives an equal integrated torque for both propellers. No general solution can be given for this blade-angle difference because the problem is complicated by the distribution of load and solidity. A few conclusions may be drawn, however, for the differential torque at the blade elements with the aid of figure 1 and equation (23). For the front propeller, $v = 0$ and therefore $\varphi_1 > \varphi_2$. By equation (28), $C_{L_1} > C_{L_2}$ and thus $\alpha_1 > \alpha_2$ and $\theta_1 > \theta_2$. For equal torque, therefore, θ_2 must be less than θ_1 at each radius. If θ_2 is not correctly set, however, the torque on the rear element may be greater or less than on the front. (See figs. 5 and 6.)

APPLICATION OF METHOD TO EIGHT-BLADE DUAL PROPELLER

The foregoing method has been applied to the calculation of the performance of an eight-blade dual propeller with Hamilton Standard 3155-6 and 3156-6 blades. A description of this propeller and results of wind-tunnel tests are given in references 5 and 6. The lift and the lift-drag curves are given in figures 3 and 4, respectively. The section characteristics for $x = 0.6$, 0.7, 0.8, 0.9, and 0.95 were taken from figure 10 of reference 7 for the appropriate thicknesses. At $x = 0.2$, the section is almost circular; it was, therefore, assumed to be operating at zero lift and a constant C_D of 0.4. At $x = 0.3$, the section is almost symmetrical and quite thick. This section was arbitrarily given a C_D of 0.05 and a slope of lift curve of 0.045 per degree with zero lift at $\alpha = 0$. The characteristics for $x = 0.2$ and 0.3 are quite rough approximations but should be satisfactory inasmuch as the contributions of these elements are small.

The determination of the characteristics for the section at $x = 0.45$ was somewhat more involved. It was first

necessary to reconstruct the profile from the drawings. This section was found to have double camber, with a mean camber of 3.8 percent and a thickness of 16.6 percent. By an unpublished method for determining the characteristics of a family of airfoils based upon a given thickness and camber distribution, an example for the Clark Y airfoils was prepared. From this example the section at $x = 0.45$ was found to have an angle of zero lift of -3.3° and a slope of lift curve of 0.094 per degree. The lift-drag ratios were taken to be the same as those for the 16.6-percent-thick Clark Y airfoil of figure 10 of reference 7. This choice is not quite correct, but the error thus introduced into the calculations is very small. The values of F used were those for the four-blade propeller. (See fig. 15.)

The differential-torque curves for the front and rear propellers at $x = 0.7$, $\theta_1 = 46.6^\circ$, and $\theta_2 = 45.6^\circ$ are given in figure 5. This condition corresponds to a blade-angle setting of 45° and 44° at 0.75 radius. Similar curves were constructed for the other radii and also for the differential thrust. Figures 6 and 7 give the differential-thrust and the differential-torque distribution, respectively, for the same blade setting at $J = 2.15$, corresponding to equal torque. Similar distributions were determined for other values of advance-diameter ratio and of blade angle. The calculated individual thrust and individual power curves are given in figures 8 and 9, respectively, for the 30°, 45°, and 60° settings of the front propeller with the same values of the rear propeller used in references 5 and 6. Comparisons between the calculated and the observed power coefficients for the front and for the rear propellers are provided in figures 10 and 11, respectively. Figures 12 and 13 provide similar comparisons for the total thrust and the total power coefficients. The extent of the calculated curves is limited by the fact that calculations were carried out only as far as $C_L = 0.8$ for the front propeller.

Examination of these figures indicates a quite good agreement between the calculated and the observed curves, especially for the power coefficient for the rear propeller. The power of the front propeller does not show so good an agreement — the reason is not at present apparent. The individual thrust curves were not obtained experimentally and could not, therefore, be compared. The total

thrust seems to agree quite well but shows the same discrepancies as the total power curves. Further calculations of this type for both dual and single propellers would be highly desirable.

CONCLUDING REMARKS

A method has been developed herein for calculating the performance of a dual-rotating propeller from the section characteristics of the blade elements. Computations for an eight-blade propeller are compared with the results of low-speed wind-tunnel tests of this propeller in both the tractor and the pusher positions. The computations agree within the experimental accuracy of the measurements.

Langley Memorial Aeronautical Laboratory,
National Advisory Committee for Aeronautics,
Langley Field, Va.,

APPENDIX A

METHOD OF COMPUTATION

The complete performance of a dual propeller for any particular radius may be calculated on three work sheets, samples of which are included. (See computation forms.) Sheet 1 is used to determine the lift coefficients, the inflow angles, and the advance-diameter ratio for the two propellers. Sheet 2 is a trial sheet necessary in determining the lift coefficient on the rear propeller. Sheet 3 provides the computation of the differential-thrust and the differential-torque coefficients for both propellers.

Sheet 1.- For any particular radius x, the solidity σ and the blade angles θ_1 and θ_2 are specified. Arbitrary values of C_{L_1} at intervals of 0.1, for example, are selected and the angle of attack α_1 is determined from the lift curve (infinite aspect ratio). Most entries are self-evident; the others are obtained as follows:

$\varphi_1 = \theta_1 - \alpha_1$. The value of F_1 is determined from charts for the appropriate values of x and φ_1. Values of F are given in figures 14 and 15 for three- and four-blade propellers, respectively. Similar charts for two- and six-blade propellers may be found in reference 7. The original data for these charts were obtained from reference 8. Then, from equation (1),

$$\tan \epsilon_1 = \frac{C_{L_1} \frac{\sigma}{4F_1}}{\sin \varphi_1}$$

from equations (10) and (11),

$$A = \frac{\omega F_1 \tan \epsilon_1}{\cot \varphi_1 + \tan \epsilon_1}$$

and, by equation (21),

$$G = \frac{\omega \tan (\varphi_1 - \epsilon_1) + A \cot \varphi_1}{1 + 2A}$$

Sheet 1 is left temporarily and sheet 2 used.

Sheet 2.— It is now necessary to determine the value of C_{L_2} at which the rear propeller operates when the front propeller operates at the assumed value of C_{L_1}. This value may be most conveniently determined by assuming two values of $\theta_2 - \varphi_2$ and determining the corresponding values of C_{L_2}, plotting them directly on the chart of C_L against α and determining the intersection of the lift curve with the line connecting these two points. The function C_{L_2} against $\theta_2 - \varphi_2$ is really a curve but, if the points are taken close together, the straight line is sufficiently accurate.

The sheet starts with the assumed value of $\theta_2 - \varphi_2$; $\varphi_2 = \theta_2 - (\theta_2 - \varphi_2)$; F_2 is obtained from the F--chart for the appropriate radius and φ; by equation (22),

$$\tan \epsilon_2 = \frac{\tan \varphi_2 - G}{1 - F_2 + G \tan \varphi_2}$$

and, from equation (1),

$$C_{L_2} = \frac{\sin \varphi_2 \tan \epsilon_2}{\sigma / 4F_2}$$

The lower half of sheet 2 provides space for the second computation at another value of $\theta_2 - \varphi_2$.

The intersection determines a value of C_{L_2} and $\alpha_2 = \theta_2 - \varphi_2$. These values are used in the return to sheet 1.

Sheet 1 (continued).- Computations similar to the first part of sheet 1 are repeated for the rear propeller as far as ϵ_2. The additional indicated tabulations are entered with the value calculated by equation (23) as

$$\tan \varphi_{02} = (1 + 2A) \tan (\varphi_2 - \epsilon_2) - A \cot \varphi_1$$

$$J = \pi x \tan \varphi_0$$

Sheet 3.- All the information required to compute the differential thrust and the differential torque is now at hand. These computations are performed as indicated. The lift coefficient and several other entries have been repeated for convenience. From the L/D curves,

$$\tan \gamma_1 = C_D / C_L$$

by equation (25a).

$$\frac{dC_{Q_1}}{dx} = \frac{\pi^3 x^4 F_1}{2} \frac{\tan \epsilon_1 (1 + \cot \varphi_1 \tan \gamma_1)}{(\cot \varphi_1 + \tan \epsilon_1)^3}$$

and, by equation (24a),

$$\frac{dC_{T_1}}{dx} = \pi^3 x^3 F_1 \frac{\tan \epsilon_1 (\cot \varphi_1 - \tan \gamma_1)}{(\cot \varphi_1 + \tan \epsilon_1)^2}$$

The coefficients for the rear propeller are similarly determined from equation (25b) as

$$\frac{dC_{Q_2}}{dx} = \frac{\pi^3 x^4 F_2}{2} \frac{\tan \epsilon_2 (1 + \cot \varphi_2 \tan \gamma_2)}{[(\cot \varphi_2 + \tan \epsilon_2)/(1 + 2A)]^3}$$

and, from equation (24b), as

$$\frac{dC_{T_2}}{dx} = \pi^3 x^3 F_2 \frac{\tan \epsilon_2 (\cot \varphi_2 - \tan \gamma_2)}{[(\cot \varphi_2 + \tan \epsilon_2)/(1 + 2A)]^2}$$

When these computations have been completed, the differential thrust and the differential torque may be plotted as a function of J for each radius, then cross-plotted as a function of radius for a given J and integrated (figs. 5 to 7).

Limiting case.- For $C_L = 0$, $\tan \epsilon = 0$, $\tan \gamma = \infty$, and equations (24) and (25) reduce to

$$\frac{dC_T}{dx} = -\frac{\pi^3 x^3}{4} \frac{\tan \varphi_0}{\cos \varphi_0} \sigma C_D (1 + 2A)^2$$

$$\frac{dC_Q}{dx} = \frac{\pi^3 x^4}{8} \frac{\sigma C_D}{\cos \varphi_0} (1 + 2A)^2$$

For the front propeller, $A \equiv 0$; for the rear propeller, $A = 0$ only if $C_{L_1} = 0$.

DESIGN FOR EQUAL TORQUE

The condition for equal torque is given as

$$C_{L_1}/\sin \varphi_1 = C_{L_2}/\sin \varphi_2$$

or

$$F_1 \tan \epsilon_1 = F_2 \tan \epsilon_2$$

With F_1 and ϵ_1 determined from sheet 1 for a given blade-angle setting θ_1, the blade angle θ_2 required for equal torque may be found in the following manner:

$$F_2 = \frac{F_1 \tan \epsilon_1}{\tan \epsilon_2}$$

where

$$\tan \epsilon_2 = \cot \varphi_1 + (1 + 2F_1) \tan \epsilon_1 - \cot \varphi_2$$

A value of φ_2 is assumed and F_2 calculated. This calculated value is compared with that obtained from the F-chart for the given values of B, φ, and x. Successive values are assumed until agreement is reached. In practice the process is found to be rapidly convergent.

With both φ_2 and ϵ_2 determined, values of C_{L_2}, α_2, and θ_2 immediately follow.

APPENDIX B

DERIVATION OF EXPRESSIONS FOR INTERFERENCE VELOCITIES AND DIFFERENTIAL THRUST AND DIFFERENTIAL TORQUE

Interference Velocities

$$\tan \epsilon = \frac{w}{W} = \frac{w \cos \varphi}{r\Omega + v - w \sin \varphi}$$

and

$$\tan \varphi = \frac{V + u + w \cos \varphi}{r\Omega + v - w \sin \varphi}$$

Now

$$u_1 = F_2 w_2 \cos \varphi_2 \qquad (6)$$

and

$$F_2 \tan \epsilon_2 = \frac{F_2 w_2 \cos \varphi_2}{r\Omega_2 + v_2 - w_2 \sin \varphi_2}$$

$$= \frac{u_1}{r\Omega_2 + v_2} \frac{r\Omega_2 + v_2 - w_2 \sin \varphi_2 + w_2 \cos \varphi_2 \tan \varphi_2}{r\Omega_2 + v_2 - w_2 \sin \varphi_2}$$

$$= \frac{u_1}{r\Omega_2 + v_2} (1 + \tan \varphi_2 \tan \epsilon_2)$$

Thus,

$$\frac{u_1}{r\Omega_2 + v_2} = \frac{F_2 \tan \epsilon_2}{1 + \tan \varphi_2 \tan \epsilon_2} \qquad (7)$$

Similarly,

$$\frac{u_2}{r\Omega_1} = \frac{F_1 \tan \epsilon_1}{1 + \tan \varphi_1 \tan \epsilon_1}$$

$$= \frac{F_1 \tan \epsilon_1 \cot \varphi_1}{\cot \varphi_1 + \tan \epsilon_1}$$

$$= A' \cot \varphi_1$$

And,

$$\frac{u_2}{r\Omega_2} = \frac{u_2}{r\Omega_1} \frac{\Omega_1}{\Omega_2}$$

$$= A'\omega \cot \varphi_1$$

$$= A \cot \varphi_1 \qquad (8)$$

Also,

$$v_2 = 2F_1 w_1 \sin \varphi_1$$

$$= 2F_1 w_1 \cos \varphi_1 \tan \varphi_1$$

$$= 2u_2 \tan \varphi_1$$

Therefore,

$$\frac{v_2}{r\Omega_2} = 2A \qquad (9)$$

Differential Thrust and Differential Torque

The differential thrust and the differential torque are given as

$$dT = BX \, dr$$

and

$$dQ = BY\, r\,dr$$

where

$$X = L \cos\varphi - D \sin\varphi$$

and

$$Y = L \sin\varphi + D \cos\varphi$$

or, in the usual coefficient form,

$$C_X = C_L \cos\varphi - C_D \sin\varphi$$

$$= C_L \sin\varphi \,(\cot\varphi - \tan\gamma)$$

$$C_Y = C_L \sin\varphi \,(1 + \cot\varphi \tan\gamma)$$

where

$$\tan\gamma = C_D/C_L$$

In terms of the usual nondimensional coefficients, the differential thrust and the differential torque become

$$\frac{dC_T}{dx} = \frac{\pi^3 x^3}{4} \frac{W^2}{r^2\Omega^2} \sigma C_X$$

$$\frac{dC_Q}{dx} = \frac{\pi^3 x^4}{8} \frac{W^2}{r^2\Omega^2} \sigma C_Y$$

where σ is the solidity at the radius r.

The expression for W is obtained as

$$W = (V + u + w\cos\varphi)\csc\varphi$$

$$= r\Omega \frac{V + u + w\cos\varphi}{r\Omega} \csc\varphi$$

Now

$$\frac{r\Omega + v}{V + u + w \cos \varphi} = \frac{r\Omega + v - w \sin \varphi + w \sin \varphi}{V + u + w \cos \varphi} = \cot \varphi + \tan \epsilon$$

For the front propeller,

$$r\Omega + v = r\Omega_1$$

For the rear propeller

$$r\Omega + v = r\Omega_2 + v_2 = r\Omega_2(1 + 2A)$$

Therefore,

$$W_1 = r\Omega_1 \frac{\csc \varphi_1}{\cot \varphi_1 + \tan \epsilon_1}$$

$$W_2 = r\Omega_2 \frac{\csc \varphi_2 (1 + 2A)}{\cot \varphi_2 + \tan \epsilon_2}$$

Also

$$\sigma C_L = 4F \sin \varphi \tan \epsilon$$

The differential thrust and the differential torque are then obtained as

$$\frac{dC_T}{dx} = \pi^3 x^3 \frac{F \tan \epsilon (\cot \varphi - \tan \gamma)}{[(\cot \varphi + \tan \epsilon)/(1 + 2A)]^2} \qquad (24)$$

$$\frac{dC_Q}{dx} = \frac{\pi^3 x^4}{2} \frac{F \tan \epsilon (1 + \cot \varphi \tan \gamma)}{[(\cot \varphi + \tan \epsilon)/(1 + 2A)]^2} \qquad (25)$$

with $A \equiv 0$ for the front propeller.

REFERENCES

1. Lock, C. N. H.: Interference Velocity for a Close Pair of Contra-Rotating Airscrews. 5234. A.P. 270, N.P.L. (British), July 22, 1941.

2. Collar, A. R.: On the Periodic Effects Experienced by the Blades of a Contra-Rotating Airscrew Pair. R. & M. No. 1995, British A.R.C., 1941. 1941.

3. Collar, A. R.: A Note on the Static Thrust of Contra-Rotating Airscrews. R. & M. No. 1994 British A.R.C., 1941.

4. Goldstein, Sydney: On the Vortex Theory of Screw Propellers. Proc. Roy. Soc. (London), ser. A., vol. 123, no. 792, April 6, 1929, pp. 440-465.

5. Biermann, David, and Gray, W. H.: Wind-Tunnel Tests of Eight-Blade Single- and Dual-Rotating Propellers in the Tractor Position. NACA A.R.R., Nov. 1941.

6. Biermann, David, and Gray, W. H.: Wind-Tunnel Tests of Single- and Dual-Rotating Pusher Propellers Having from Two to Eight Blades. NACA A.R.R., Feb. 1942.

7. Crigler, John L., and Talkin, Herbert W.: Propeller Selection from Aerodynamic Considerations. NACA A.C.R., July 1942.

8. Lock, C. N. H., and Yeatman, D.: Tables for Use in an Improved Method of Airscrew Strip Theory Calculation. R. & M. No. 1674, British A.R.C., 1935.

COMPUTATION FORM FOR DUAL-ROTATING PROPELLERS

$x = 0.7$; $\sigma = 0.1380$; $\theta_1 = 46.6°$; $\theta_2 = 45.6°$; $\omega = 1$

Sheet 1

C_{L_1}	0.1	0.2	0.3	0.4
α_1, deg				0.57
φ_1, deg				46.03
sin φ_1				0.71970
cot φ_1				0.96468
F_1				0.672
$\sigma/4F_1$				0.05134
tan ϵ_1				0.02853
ϵ_1, deg				1.63
cot φ_1 + tan ϵ_1				0.99321
A				0.01930
1 + 2A				1.03860
A cot φ_1				0.01862
tan (φ_1 - ϵ_1)				0.97927
G				0.96080
C_{L_2}				0.408
α_2, deg				0.66
φ_2, deg				44.94
sin φ_2				0.70637
cot φ_2				1.0021
F_2				0.680
$\sigma/4F_2$				0.05074
tan ϵ_2				0.02931
ϵ_2, deg				1.68
tan (φ_2 - ϵ_2)				0.94104
(1 + 2A)tan(φ_2 - ϵ_2)				0.97736
tan φ_0				0.95874
J				2.11

Sheet 2

C_{L_1}	0.1	0.2	0.3	0.4
θ_2 - φ_2, deg				0.5
φ_2, deg				45.1
sin φ_2				0.70834
tan φ_2				1.0035
F_2				0.677
$\sigma/4F_2$				0.05096
tan φ_2 - G				0.04270
G tan φ_2 + 1 - F_2				1.28716
tan ϵ_2				0.03317
C_{L_2}				0.461
θ_2 - φ_2, deg				1.0
φ_2, deg				44.6
sin φ_2				0.70215
tan φ_2				0.98613
F_2				0.681
$\sigma/4F_2$				0.05066
tan φ_2 - G				0.02533
G tan φ_2 + 1 - F_2				1.24647
tan ϵ_2				0.02000
C_{L_2}				0.277

Sheet 3

J				2.11
C_{L_1}				0.4
tan ϵ_1				0.02853
cot φ_1				0.96468
tan γ_1				0.01689
1 + cot φ_1 tan γ_1				1.01629
$\frac{1}{2}\pi^3 x^4 F_1$				2.50139
(cot φ_1 + tan ϵ_1)^2				0.98647
dC_{Q_1}/dx				0.0735
cot φ_1 - tan γ_1				0.94779
$\pi^3 x^3 F_1$				7.14647
dC_{T_1}/dx				0.1959
C_{L_2}				0.408
tan ϵ_2				0.02931
cot φ_2				1.0021
tan γ_2				0.01667
1 + cot φ_2 tan γ_2				1.01671
$\frac{1}{2}\pi^3 x^4 F_2$				2.53116
$\left(\frac{\cot \varphi_2 + \tan \epsilon_2}{1 + 2A}\right)^2$				0.98621
dC_{Q_2}/dx				0.0765
cot φ_2 - tan γ_2				0.98543
$\pi^3 x^3 F_2$				7.23152
dC_{T_2}/dx				0.2118

L-330

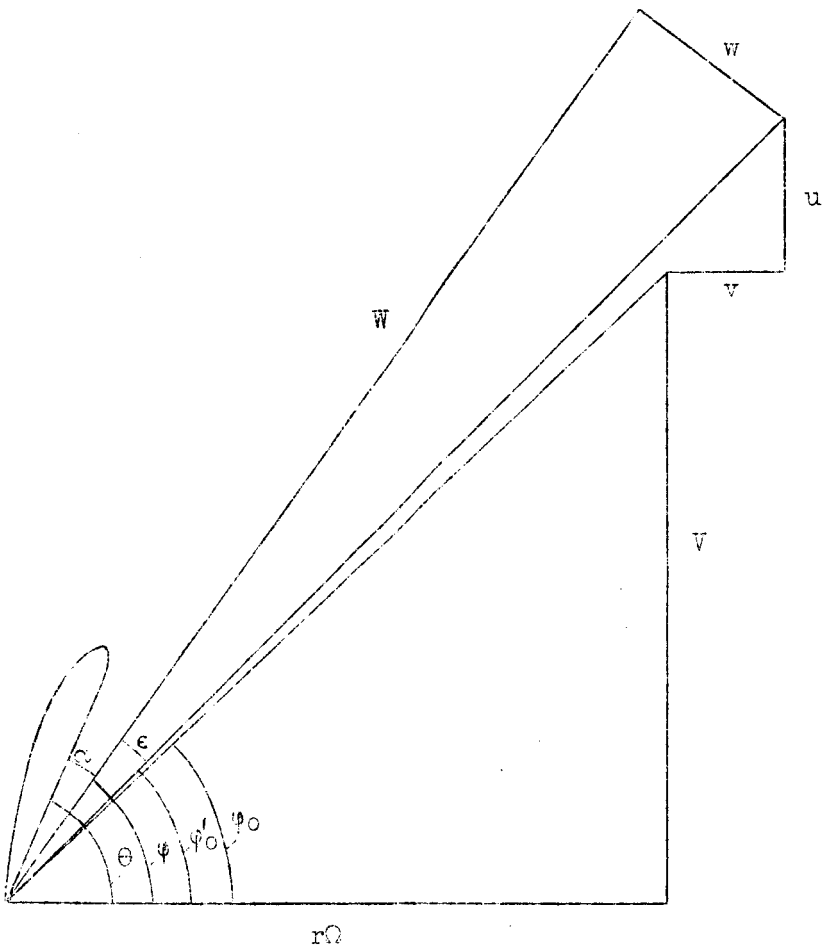

Figure 1.- Velocity diagram for propeller blade element.

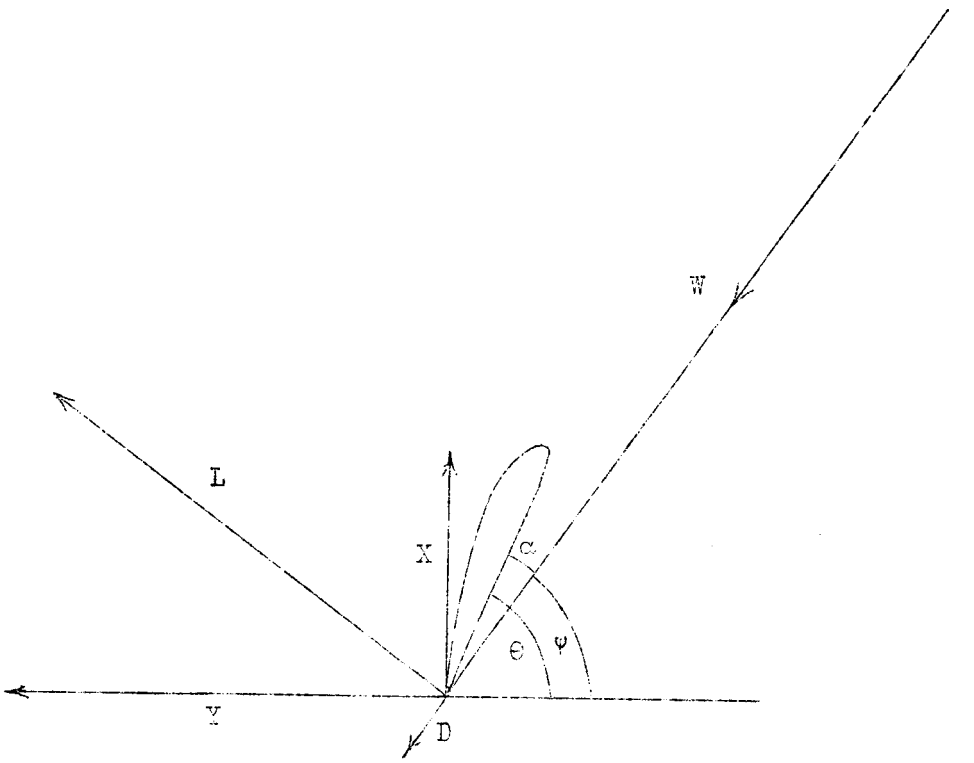

Figure 2.- Force diagram for propeller blade element.

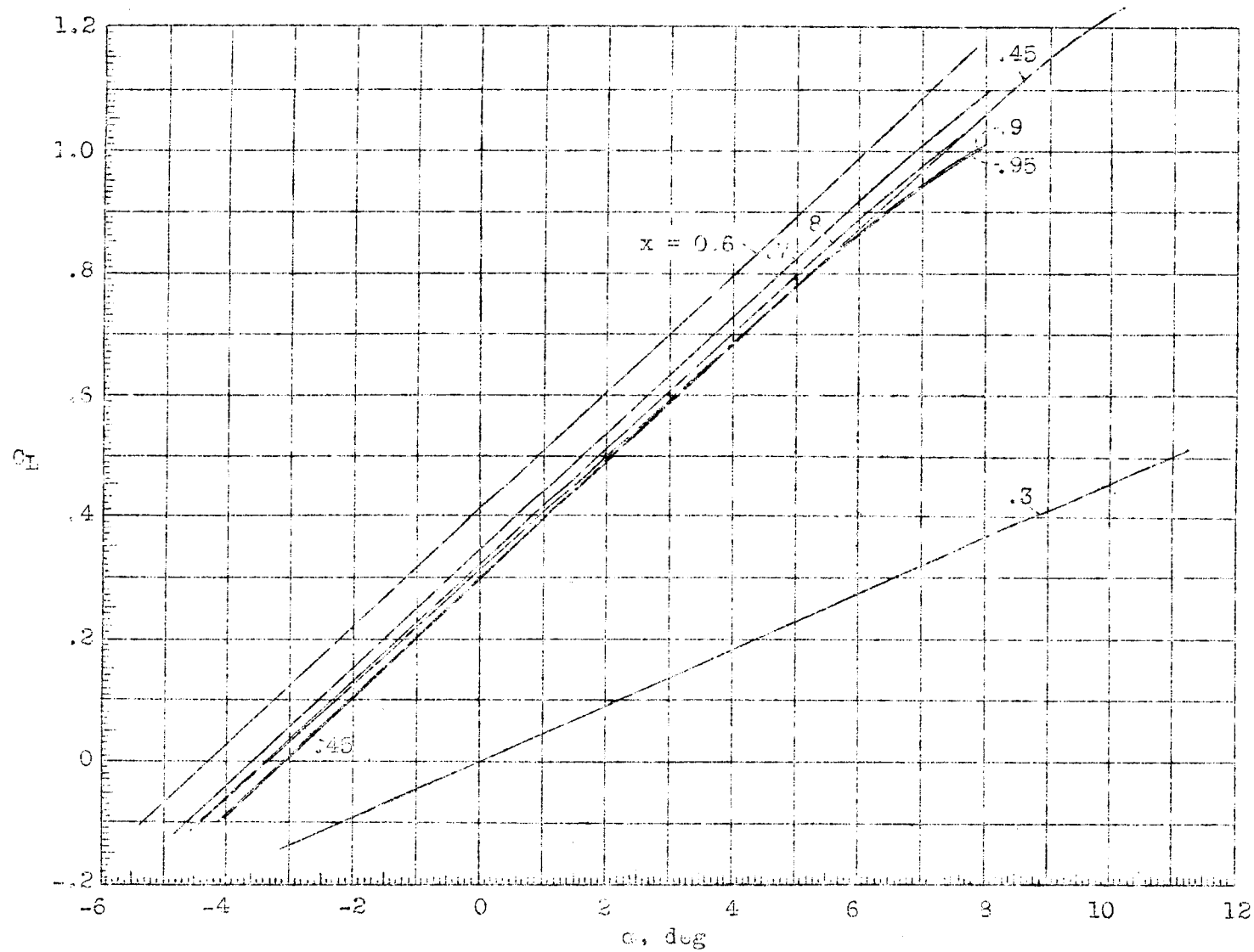

Figure 3.- Lift curves used at each station. Infinite aspect ratio. (Data from figure 10 of reference 7, except for x = 0.3.)

L-330

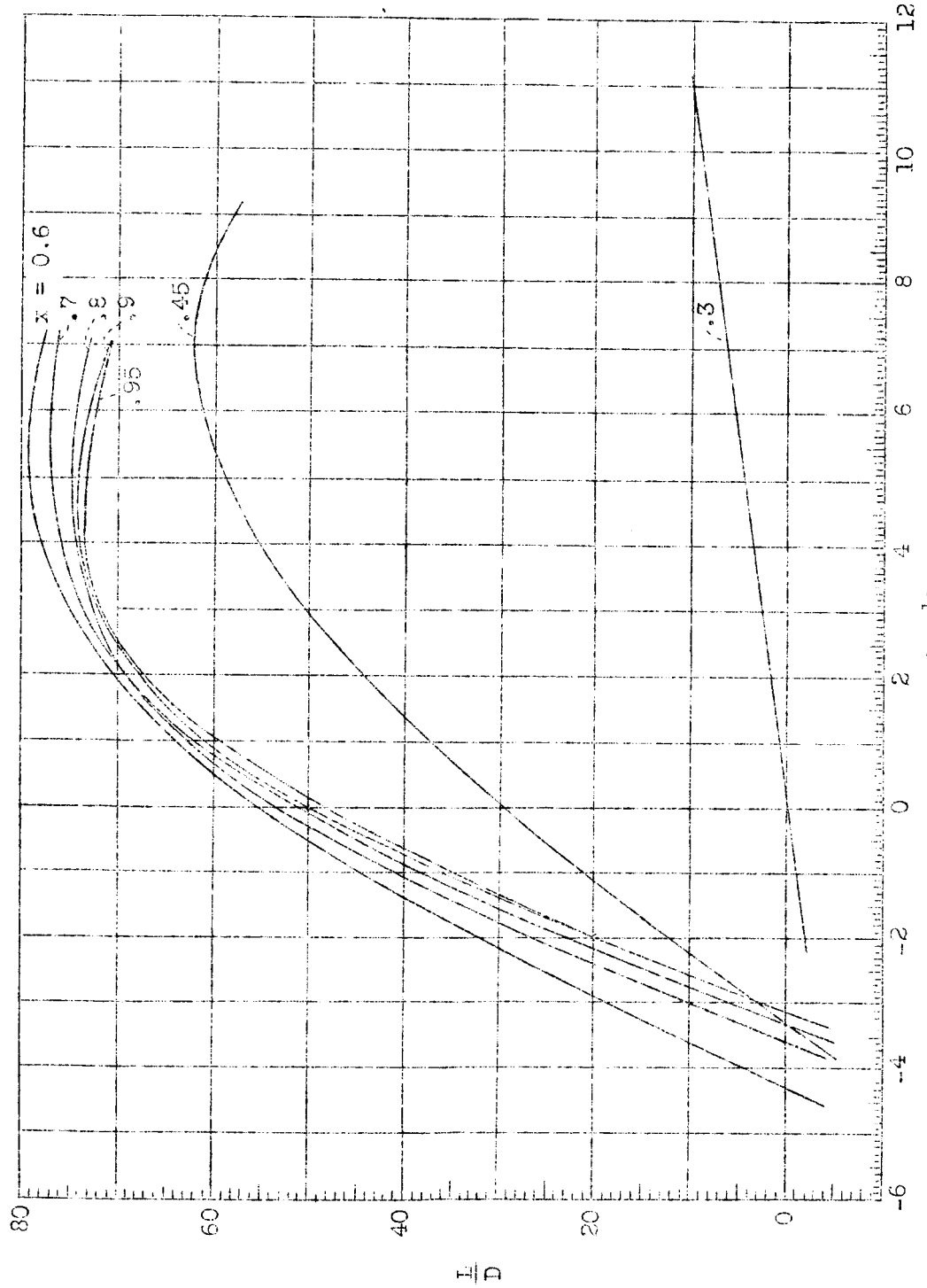

Figure 4.- Lift-drag curves used at each station. Infinite aspect ratio. (Data from figure 10 of reference 7, except for x = 0.3.)

L-330

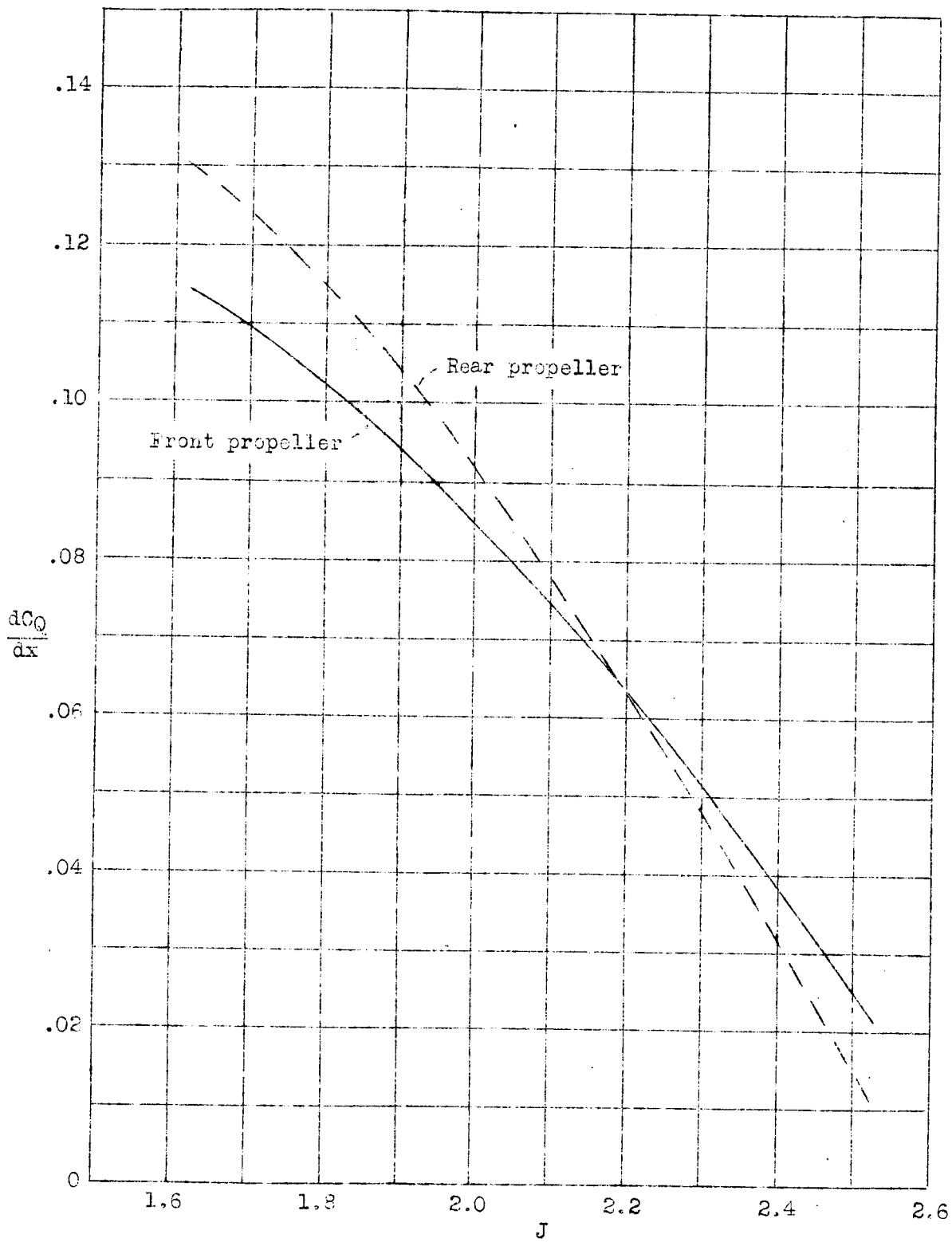

Figure 5.- Individual differential-torque curves for eight-blade dual-rotating propeller. $x = 0.7$; $\theta = 46.6^\circ$; $\theta_2 = 45.6^\circ$.

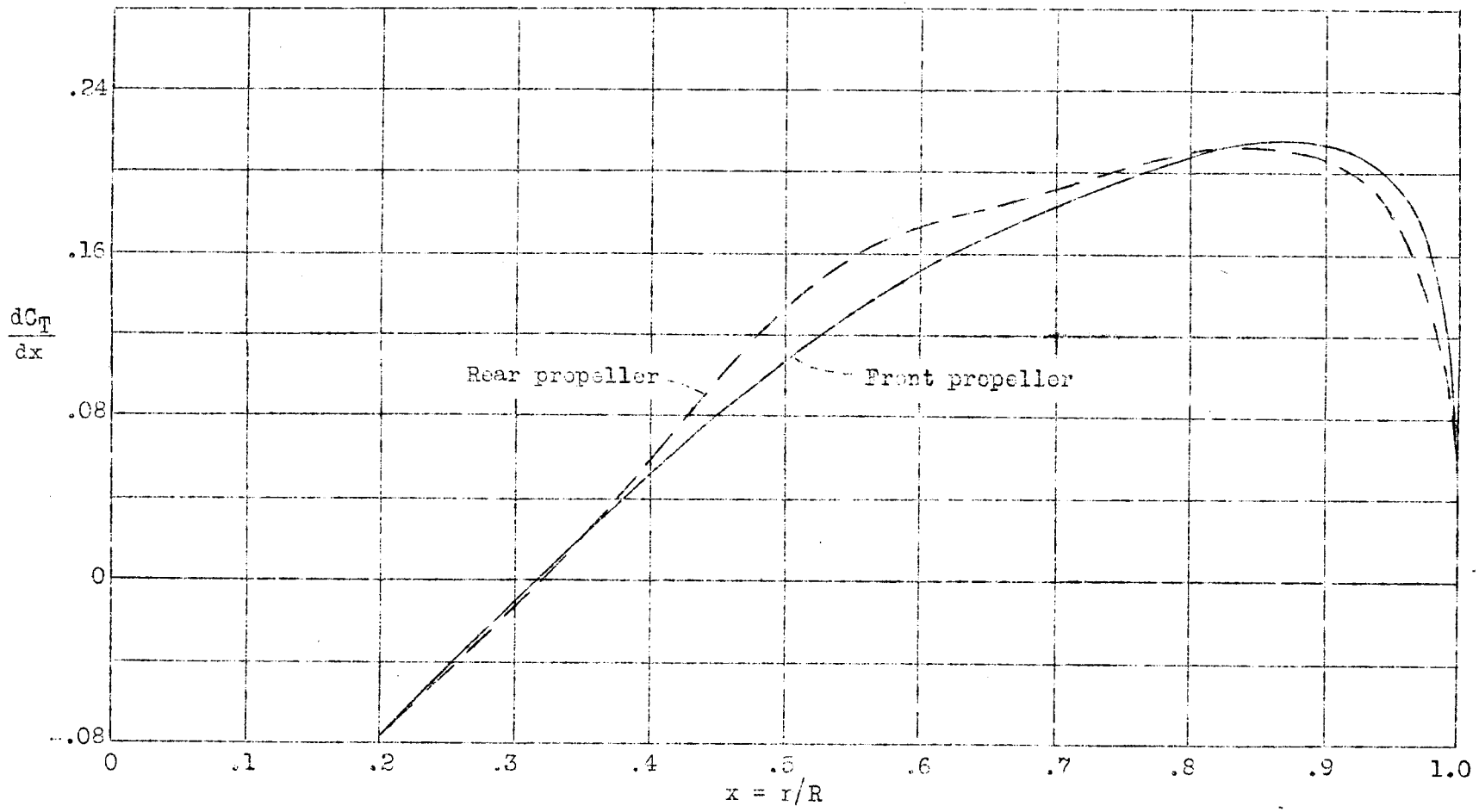

Figure 6.- Differential thrust-distribution for eight-blade dual-rotating propeller. $\beta_1 = 45^\circ$; $\beta_2 = 44^\circ$; $J = 2.15$; $C_{T_1} = 0.0947$; $C_{T_2} = 0.0993$.

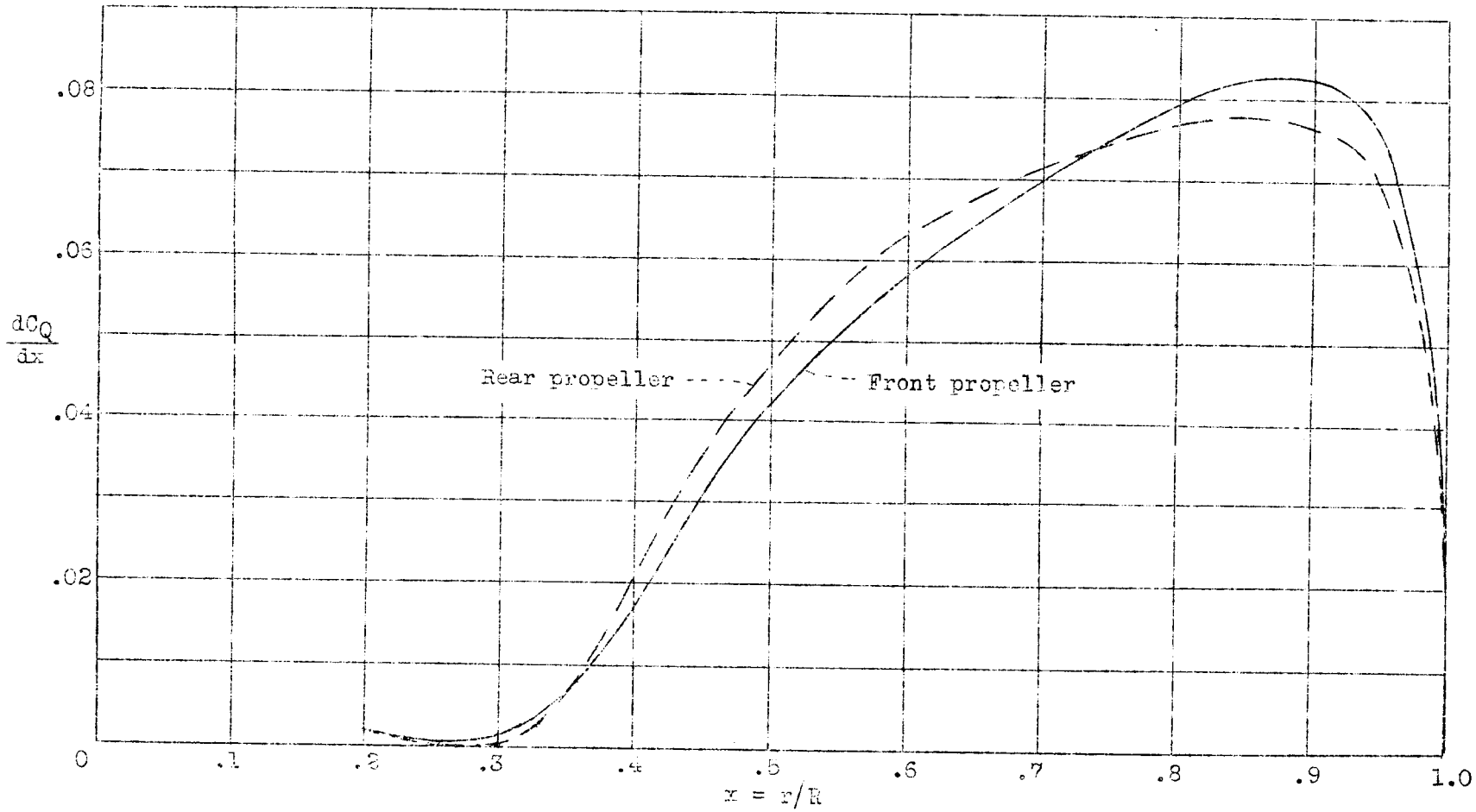

Figure 7.- Differential-torque distribution for eight-blade dual-rotating propeller. $\beta_1 = 45^\circ$; $\beta_2 = 44^\circ$; $J = 2.15$; $C_{Q_1} = C_{Q_2} = 0.0383$.

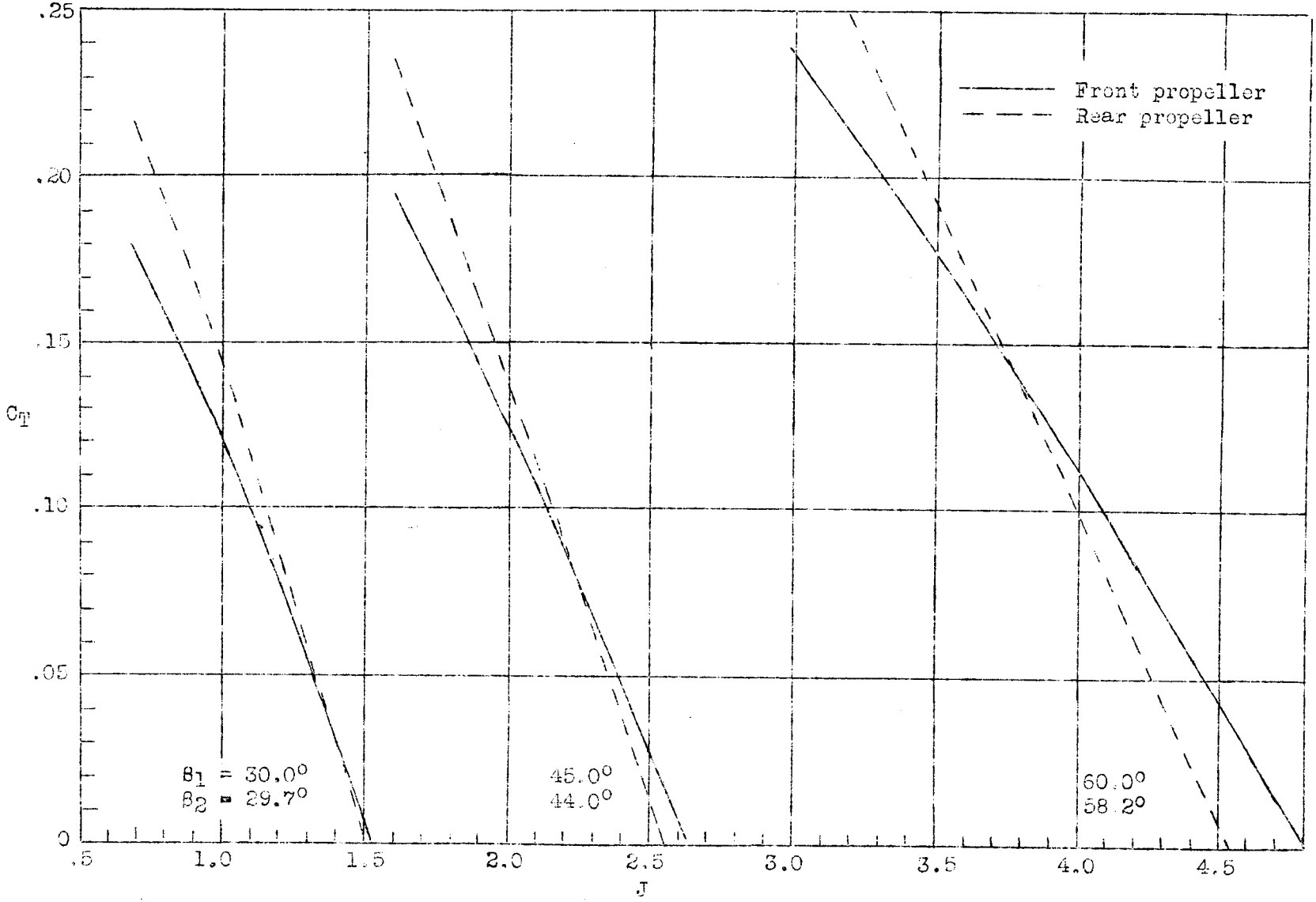

Figure 8.- Calculated individual thrust coefficient for eight-blade dual-rotating propeller.

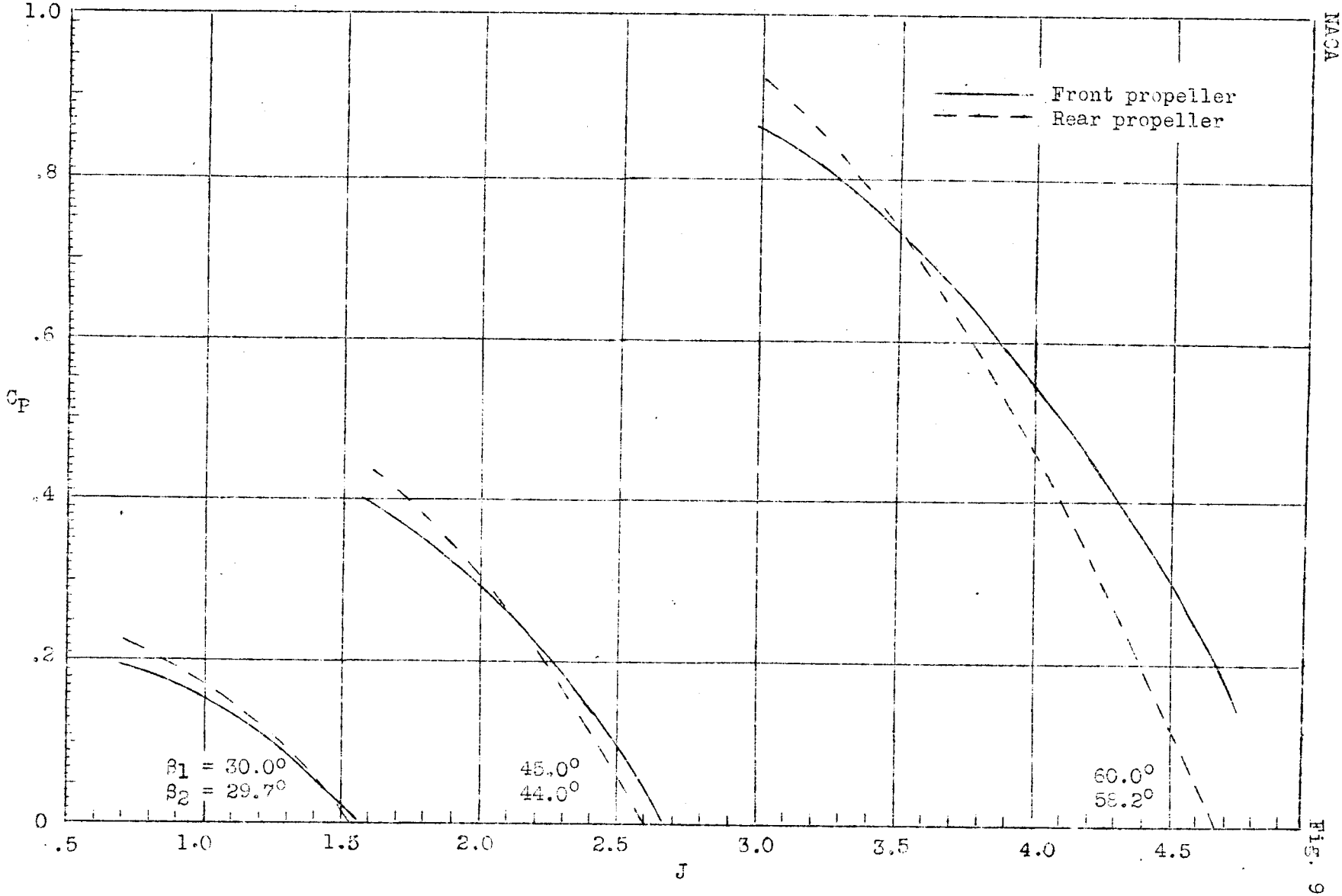

Figure 9.- Calculated individual power coefficient for eight-blade dual-rotating propeller.

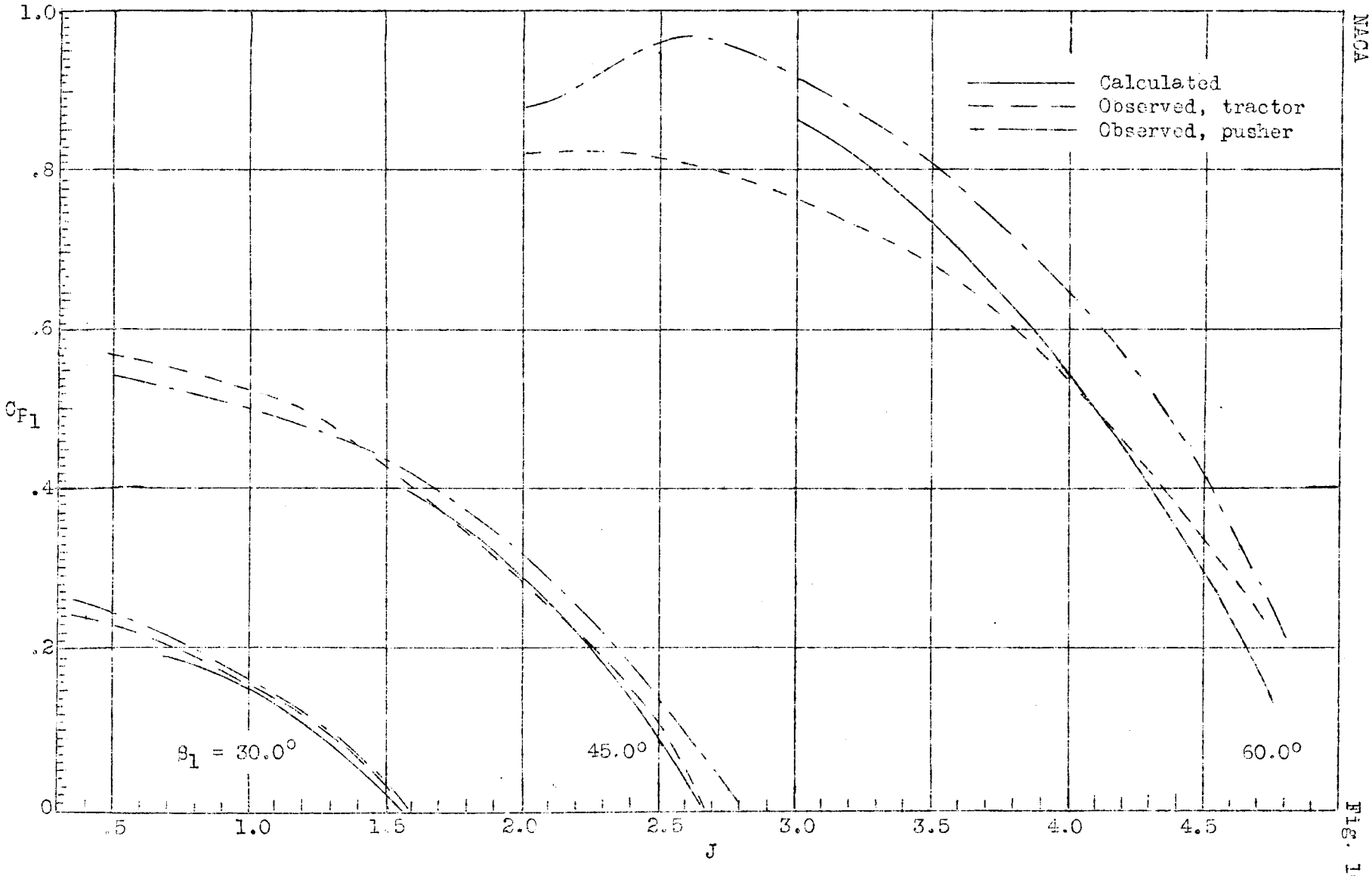

Figure 10.- Comparison of calculated and observed power coefficient for front propeller, eight-blade dual-rotation.

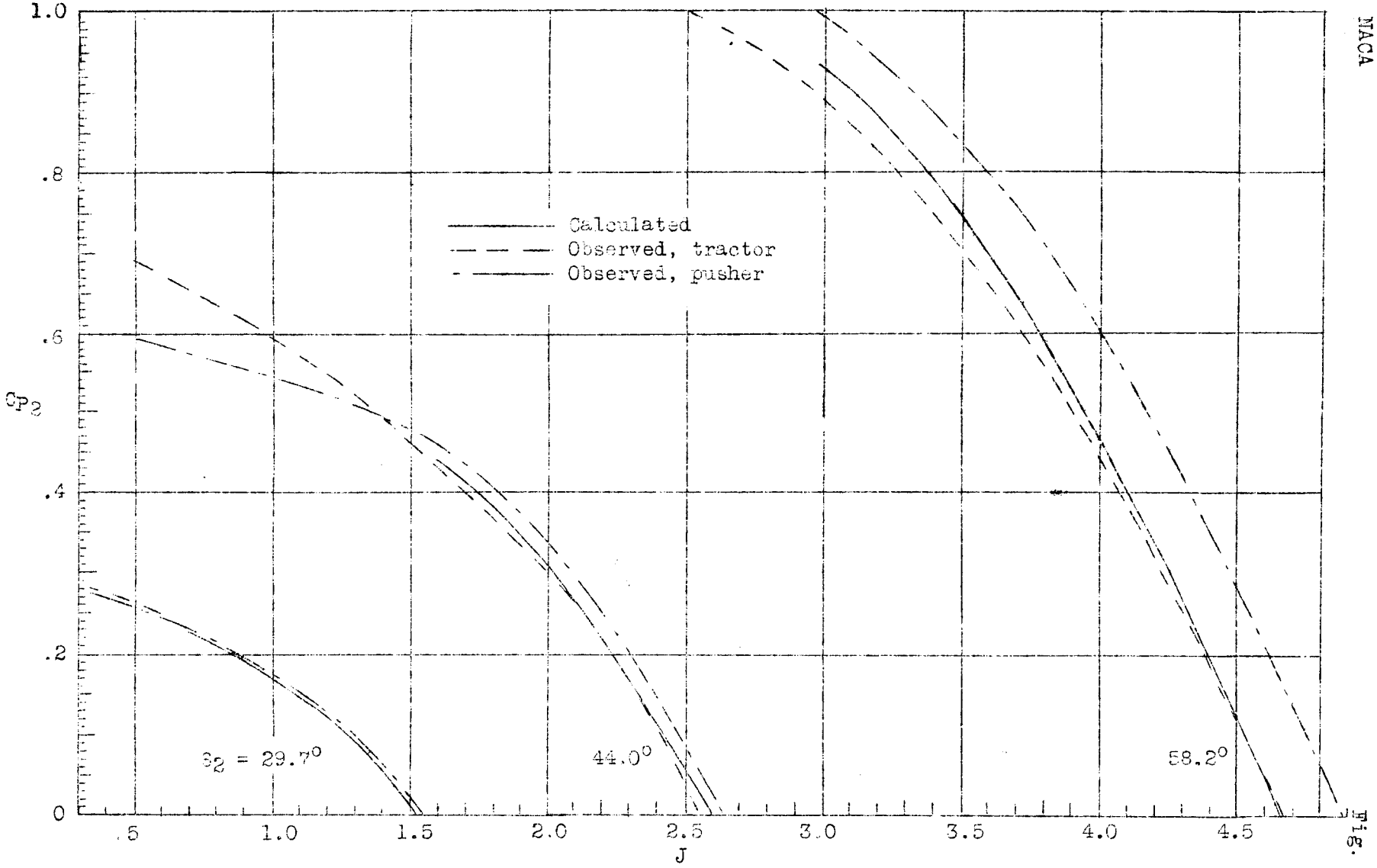

Figure 11.- Comparison of calculated and observed power coefficient for rear propeller, eight-blade dual rotation.

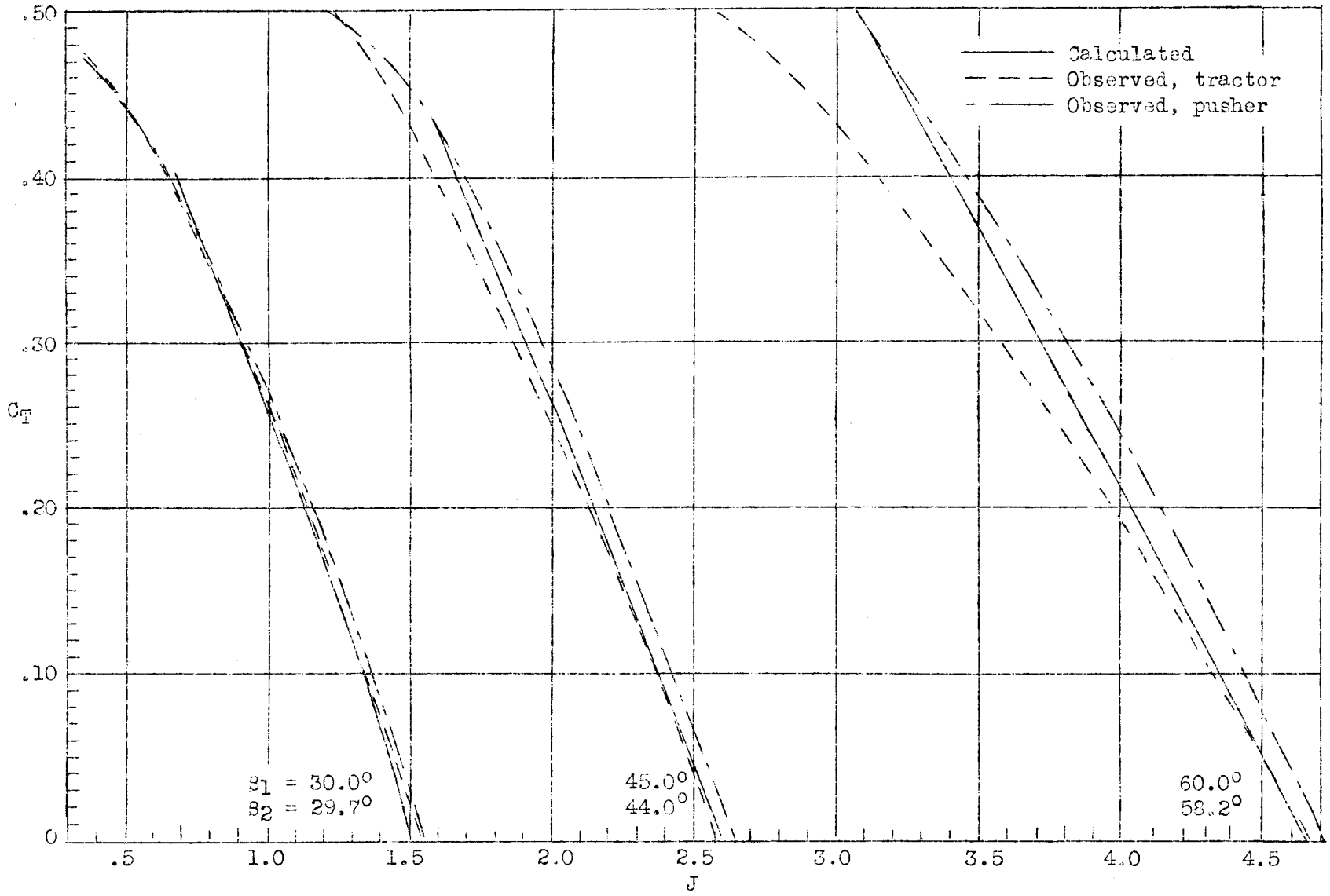

Figure 12.- Comparison of calculated and observed thrust coefficient for eight-blade dual-rotating propeller.

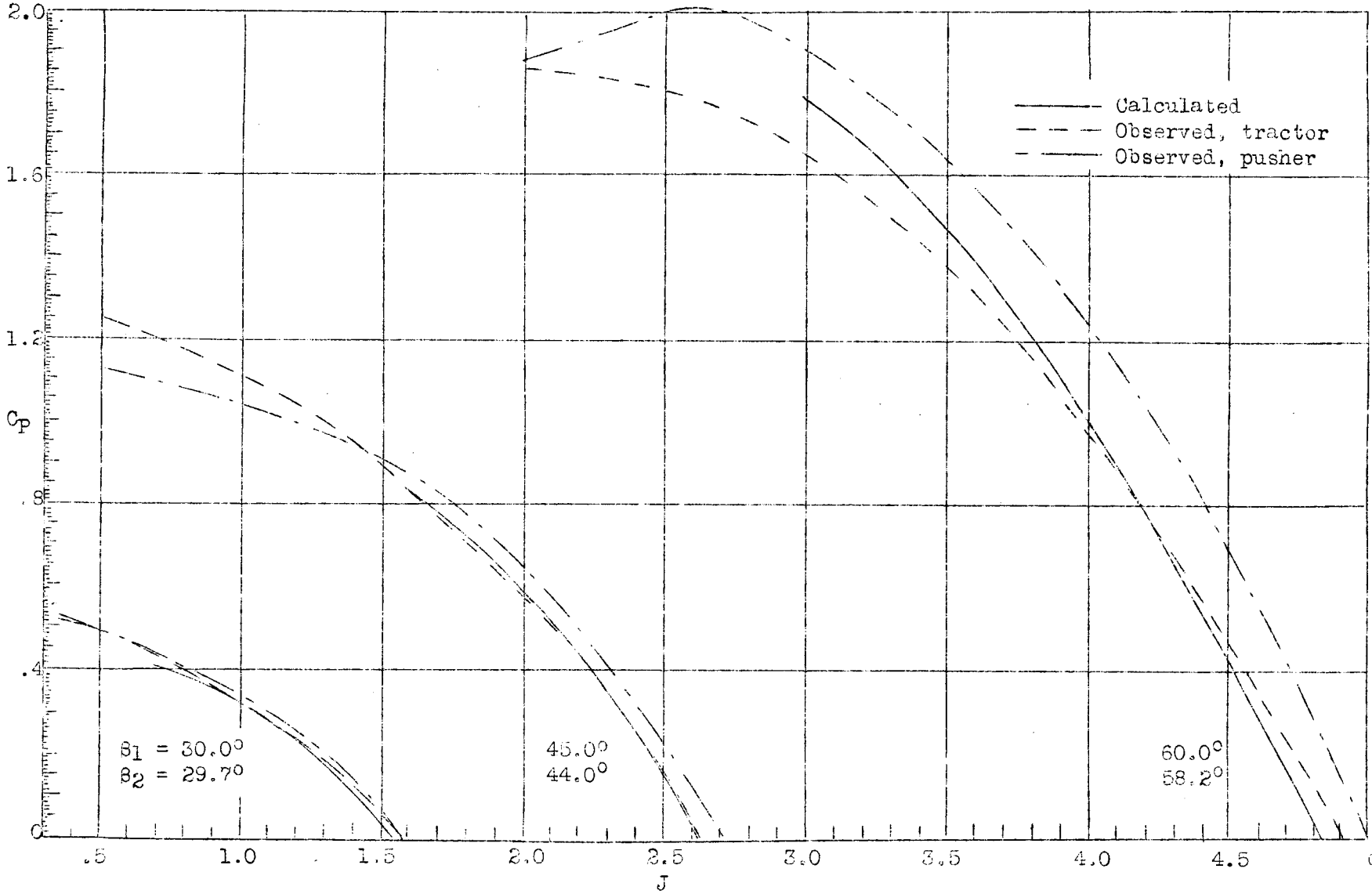

Figure 13.- Comparison of calculated and observed power coefficient for eight-blade dual-rotating propeller.

Fig. 14

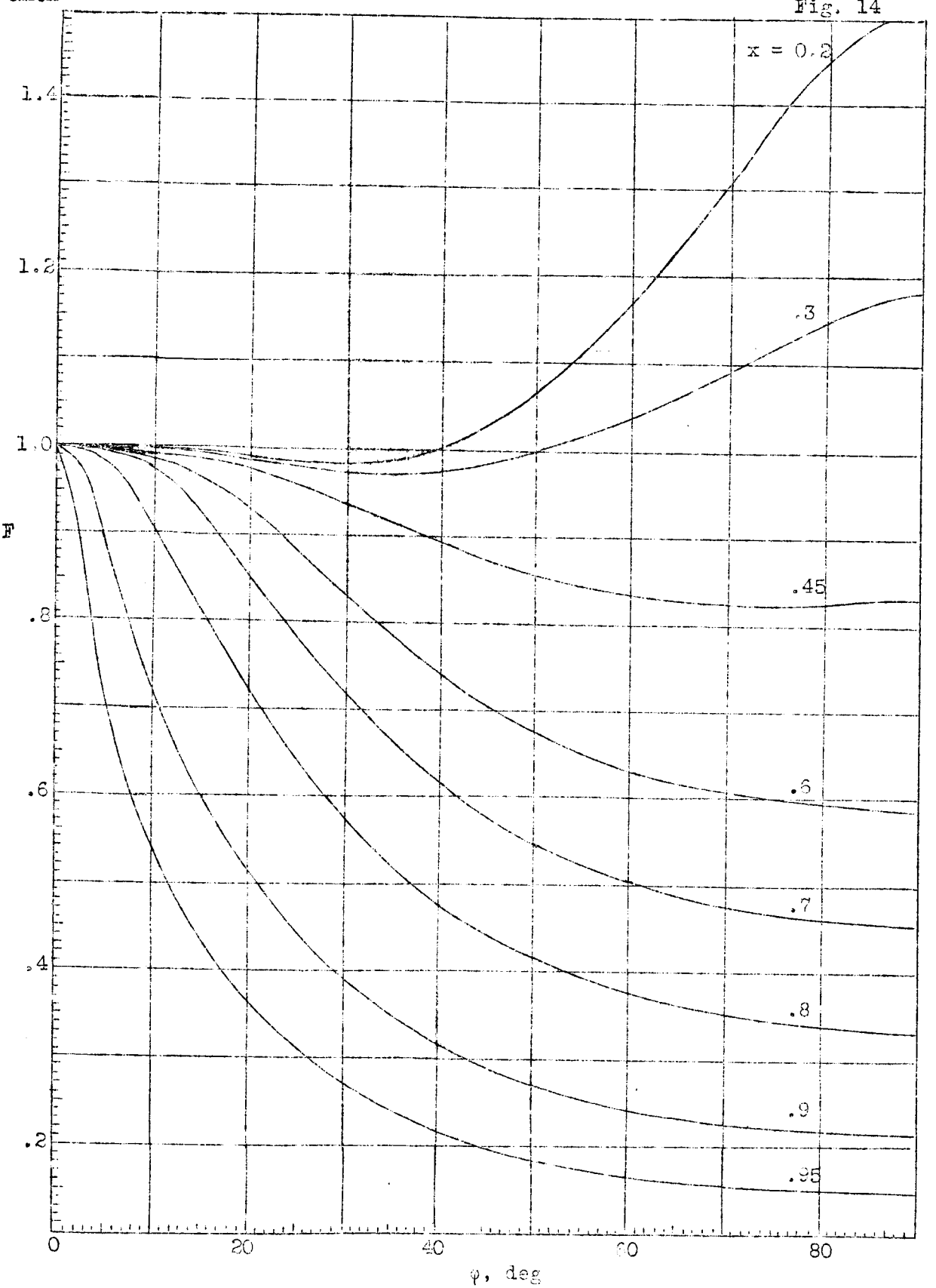

Figure 14.- Values of F for three-blade propeller. (Taken from reference 7.)

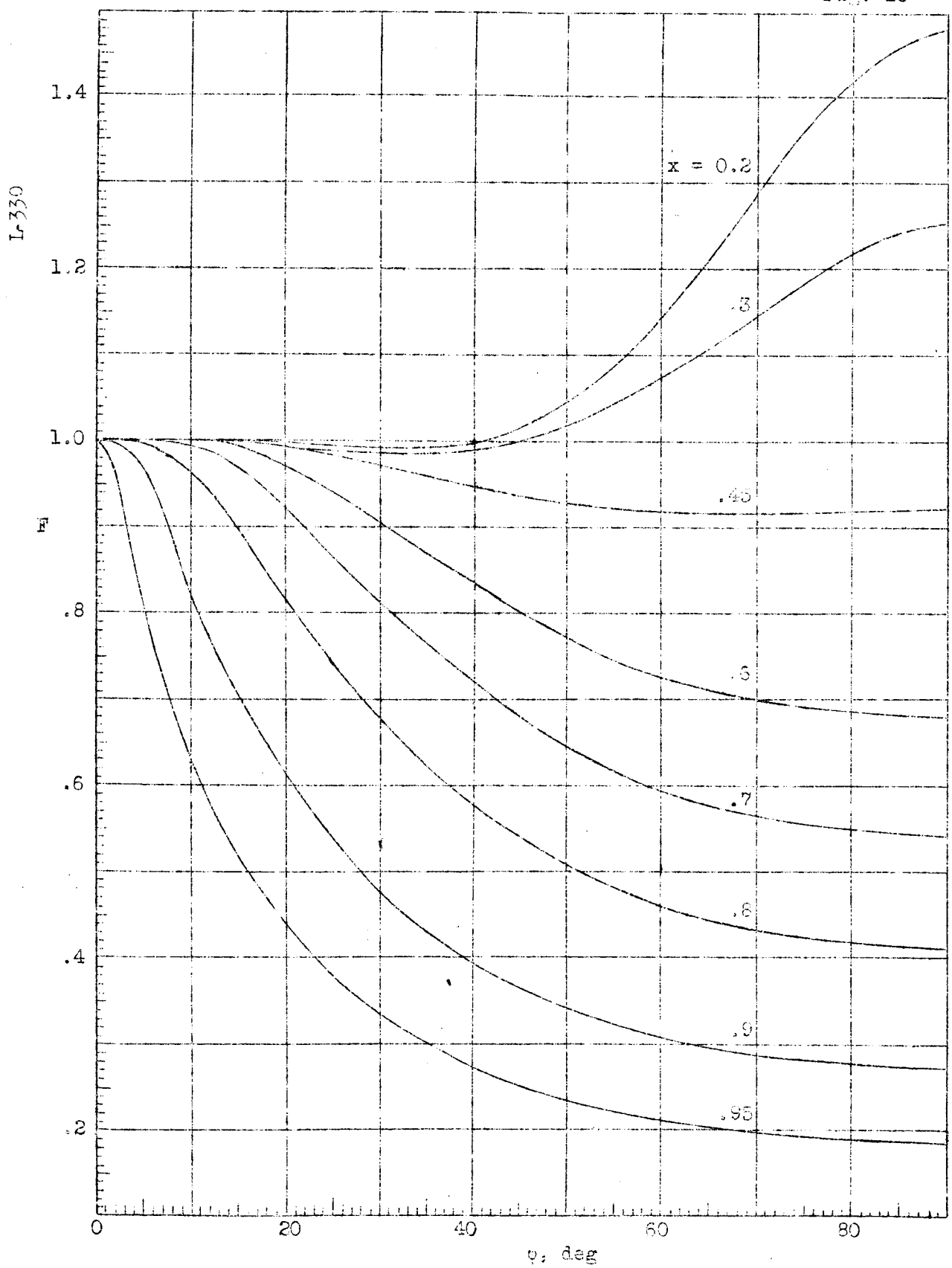

Figure 15.- Values of F for four-blade propeller. (Taken from reference 7.)